

# Covariant Holographic Entropy Cone

---

**Bowen Zhao**

*Beijing Institute of Mathematical Sciences and Applications, Beijing, China*

*E-mail:* [bowenzhao@bimsa.cn](mailto:bowenzhao@bimsa.cn)

**ABSTRACT:** The holographic entropy cone classifies the possible entanglement structures of quantum states with a classical gravity dual. For static geometries, Bao et al. established that this cone is polyhedral by constructing a graph model from Ryu–Takayanagi (RT) surfaces on a time-symmetric slice. Extending this framework to general, time-dependent states governed by the Hubeny–Rangamani–Takayanagi (HRT) formula has remained an open problem, as the relevant extremal surfaces do not lie on a common spatial slice. We resolve this by constructing a graph model directly from the causal structure of entanglement wedges. By proving a key “no-short-cut” theorem, we show that minimization over graph cuts reduces to a consideration of cuts corresponding to unions of complete HRT surfaces, establishing the equivalence of the covariant and static holographic entropy cones. Consequently, all foundational results, including polyhedrality and the finite nature of entropy inequalities, extend to general holographic states.

**KEYWORDS:** AdS-CFT Correspondence, Classical Theories of Gravity, Holographic Entropy Cone

---

## Contents

<b>1</b>	<b>Introduction</b>	<b>1</b>
1.1	Notations and Assumptions	2
<b>2</b>	<b>Graph models for covariant holographic entropy cone</b>	<b>3</b>
2.1	Definition of the Graph Model	3
2.2	Basic Lemmas	4
2.3	The “No-Short-Cut” Theorem	7
2.3.1	A worked example of the induction step	10
<b>3</b>	<b>Conclusion and Outlook</b>	<b>12</b>
<b>A</b>	<b>A Review of Maximum Principles</b>	<b>13</b>
<b>A</b>	<b>Maximum Principles and Comparison for the Minimal Surface Operator</b>	<b>13</b>
A.1	Ellipticity and linear operators	13
A.2	Weak and strong maximum principles	14
A.3	The minimal surface operator	14
A.4	Weak comparison principle for $\mathcal{M}$	15
A.5	Strong comparison principle for $\mathcal{M}$	15
A.6	Geometric interpretation	16
<b>B</b>	<b>Geometric Interpretation of the Complete Graph</b>	<b>16</b>

---

## 1 Introduction

The entanglement entropy of subregions in a quantum system provides a powerful probe of its structure. For states in holographic conformal field theories with semi-classical gravitational duals, the Ryu-Takayanagi (RT) and Hubeny-Rangamani-Takayanagi (HRT) formulae ground this study in geometry [1, 2], famously equating boundary entropy with the area of a bulk extremal surface. The set of all entropy vectors for  $n$  disjoint boundary regions forms the holographic entropy cone, whose facets correspond to universal entropy inequalities constraining any dual gravitational theory.

The foundational work of Bao et al. [3] characterized this cone for states dual to static or time-symmetric bulk geometries. Their central technical achievement was constructing a graph model from the network of RT surfaces on a fixed Cauchy slice. This enabled the application of graph-theoretic max-flow/min-cut theorems, leading to a proof that the holographic entropy cone is polyhedral. A major open question is whether an analogous description exists for states dual to fully dynamical spacetimes, where entropies are computed by HRT surfaces that are not confined to a common spatial slice. Recent progress

on a minimax formulation of HRT [4] underscores this difficulty, as it requires imposing a strong "cooperating property" on candidate timelike sheets to recover a graph model.

In this work, we resolve this problem by constructing a graph model for general covariant holographic states in arbitrary spacetime dimensions. The natural approach is to promote the RT framework by partitioning the bulk spacetime using entanglement wedges rather than spatial slices. The principal obstruction is that HRT surfaces for composite regions may not lie on a common Cauchy slice, raising the concern that graph cuts built from their segments could provide artificial "short-cuts" not corresponding to any physical HRT surface.

We overcome this obstruction by proving a general "no-short-cut" theorem. Leveraging the entanglement wedge nesting property [5] and focusing arguments akin to those used in proofs of the connected wedge theorem [6–9], we show that the minimization over all graph cuts reduces to a minimization over cuts corresponding to unions of complete, non-intersecting HRT surfaces. This theorem validates the entanglement wedge-based graph model, establishing the equivalence of the covariant holographic entropy cone with its static counterpart and, consequently, proving its polyhedrality.

The paper is structured as follows. In Section 2, we construct a graph model for covariant holographic states by partitioning the bulk spacetime using entanglement wedge boundaries. Section 2.2 establishes basic geometric lemmas governing how HRT surfaces can intersect entanglement wedges. In Section 2.3 we prove the central No-Short-Cut Theorem, showing that the minimization over arbitrary graph cuts reduces to cuts corresponding to unions of complete HRT surfaces. For clarity, Section 2.3.1 presents a worked example of the induction step, where the seam bookkeeping underlying the proof is made explicit. We conclude in Section 3 with a discussion of implications and future directions.

### 1.1 Notations and Assumptions

Here we summarize the notations, conventions, and assumptions used throughout this paper.

We adopt natural units with  $\hbar = c = 1$  and set the AdS length scale  $l_{\text{AdS}} = 1$ , while keeping Newton's constant  $G_N$  explicit. Our notation follows ref. [10], using the mostly-plus metric signature.

- **Spacetime regions:** Bulk regions are denoted by script letters  $(\mathcal{U}, \mathcal{V}, \mathcal{W}, \dots)$ , while boundary regions use straight capitals  $(U, V, W, \dots)$ . The same symbol may denote either a causal diamond or its Cauchy surface, with the meaning clear from context.
- **Cauchy slices:** Bulk Cauchy slices are denoted by  $\Sigma$  with appropriate subscripts, boundary Cauchy slices by  $\hat{\Sigma}$  with subscripts. By abuse of notation,  $\Sigma$  may also refer to Cauchy slices of the conformally compactified spacetime.
- **Causal structure:** The bulk causal future/past of region  $\mathcal{V}$  is  $J^\pm[\mathcal{V}]$ ; for boundary region  $V$ , we write  $J^\pm[V]$  for bulk causal influence and  $\hat{J}^\pm[V]$  for boundary causal influence.

- **Domains of dependence:** The bulk domain of dependence of  $\mathcal{V}$  is  $\mathcal{D}[\mathcal{V}]$ ; the boundary domain of dependence of  $V$  is  $\hat{D}[V]$ . The future and past horizons of a causal domain  $V$  is  $\hat{H}^\pm[V]$ .
- **Entanglement structures:** For boundary region  $V$ , we denote the entanglement wedge by  $\mathcal{E}(V)$ , causal wedge by  $\mathcal{C}(V)$ , and HRT surface by  $\text{HRT}(V)$ .
- **Complements:** The causal complement (bulk or boundary) uses superscript  $c$ , while set-theoretic complement within a Cauchy slice uses superscript prime notation  $(')$ .

**Assumption 1.** *We assume throughout that:*

1. *The bulk spacetime  $M$  satisfies the null curvature condition;*
2. *HRRT surfaces can be found via a maximin procedure;*
3. *The spacetime is AdS-hyperbolic (the conformal compactification  $\overline{M} = M \cup \partial M$  admits a Cauchy slice);*
4. *The spacetime region between some Cauchy slice preceding  $\mathcal{E}(V_1 \cup V_2)$  and some Cauchy slice following  $\mathcal{E}(W_1 \cup W_2)$  is singularity-free.*
5. *The global boundary state is pure, ensuring that a boundary region  $V$  and its causal complement  $V'$  share the same HRT surface.*

## 2 Graph models for covariant holographic entropy cone

As outlined above, the canonical choice for partitioning the bulk spacetime in the covariant setting is via entanglement wedges. In the terminology of the minimax formulation [4], we restrict our attention to a specific canonical class of time-sheets: the boundaries of these wedges, or entanglement wedge horizons. The key observation is that candidate time-sheets composed of segments from partial entanglement horizons are necessarily dominated by those built from complete horizons. Consequently, minimizing over graph cuts reduces to analyzing configurations defined by the connectivity of entanglement wedges, allowing us to recover holographic entropies from a discrete model. In what follows, we write

$$\partial\mathcal{E}(A) = \mathcal{H}^+[A] \cup \text{HRT}(A) \cup \mathcal{H}^-[A],$$

and refer to  $\mathcal{H}^\pm[A]$  as the future/past entanglement horizons.

### 2.1 Definition of the Graph Model

We first adapt the graph model construction for static holography [3] to the covariant setting. Let  $M$  be the bulk manifold and  $A_1, \dots, A_n$  be disjoint boundary regions. The holographic entropy vector is composed of the HRT entropies  $S(A_I)$  for all nonempty composite regions  $A_I = \bigcup_{i \in I} A_i$ , where  $I \subseteq 1, \dots, n \equiv \{1, \dots, n\}$ . The corresponding HRRT surface is denoted  $\text{HRT}(A_I)$ . The union of all such entanglement horizons partitions the bulk spacetime into finitely many pieces.

We construct a weighted graph  $(\mathcal{V}, E)$  from this partition as follows:

- A vertex  $v_i \in \mathcal{V}$  is introduced for each bulk spacetime piece.
- A vertex is designated a boundary vertex and colored by index  $a$  if it is adjacent to the boundary region  $A_a$ . The purifying region is labeled  $A_{n+1}$ .
- An edge  $(v_i, v_j) \in E$  is added between two vertices if their corresponding bulk pieces share a portion of an entanglement horizon.
- The weight  $w(v_i, v_j)$  of this edge is defined as the area (divided by  $4G_N$ ) of the segment of the HRT surface that constitutes the shared horizon between the two pieces.

A cut of the graph is a partition of the vertex set  $\mathcal{V}$  into two disjoint subsets,  $\mathcal{V} = W \cup W^c$ . This corresponds to a hypersurface in the bulk assembled from partial entanglement horizons. The set of edges crossing this partition is  $C(W) = \{(w, w') \in E \mid w \in W, w' \in W^c\}$ , and its total weight is  $|C(W)| = \sum_{e \in C(W)} w(e)$ .

**Definition 2.1** (Discrete Entropy). *For a graph model  $(\mathcal{V}, E, w)$  with boundary coloring, the discrete entropy of a boundary region  $A_I$  is*

$$S^*(I) = \min_{\mathcal{V} = W \cup W^c, \partial W = I} |C(W)|, \quad (2.1)$$

where the minimization is over all cuts  $W$  such that the set of boundary vertices contained in  $W$  is precisely those colored by indices in  $I$ , i.e.,  $\partial W := \mathcal{V} \cap W = v \in \mathcal{V} \mid b(v) \in I$ .

## 2.2 Basic Lemmas

We start with stating a basic observation about HRT surfaces. The corresponding fact for RT surfaces is established in [5] by glue and past technique.

**Lemma 2.2** (No Multi-Crossing of HRT Through Entanglement Horizon). *Let  $A, B \subset \partial M$  be boundary spatial regions on a common Cauchy slice of the boundary, and let  $\gamma_A$  and  $\gamma_B$  be their corresponding HRT surfaces in a classical asymptotically AdS spacetime satisfying the null energy condition (NEC) and the usual genericity assumptions. Denote the entanglement wedge of  $B$  by  $\mathcal{E}(B)$  and its entanglement horizon by*

$$\partial\mathcal{E}(B) = \gamma_B \cup \mathcal{H}^+(B) \cup \mathcal{H}^-(B).$$

*Then  $\gamma_A$  can intersect  $\partial\mathcal{E}(B)$  at most once along each connected component. In particular,  $\gamma_A$  cannot enter, exit, and re-enter  $\mathcal{E}(B)$ .*

*Proof.* If  $A \cap B = \emptyset$ , then by entanglement wedge nesting  $\mathcal{E}(A)$  is spacelike separated from  $\mathcal{E}(B)$ , hence  $\gamma_A$  does not intersect  $\partial\mathcal{E}(B)$ .

Assume  $A \cap B \neq \emptyset$  and suppose for contradiction that along some connected component of  $\gamma_A$  there is an exit and a subsequent re-entry into  $\mathcal{E}(B)$ . See Figure 1 for an illustration. As one traverses this component from one boundary anchor to the other, crossings with

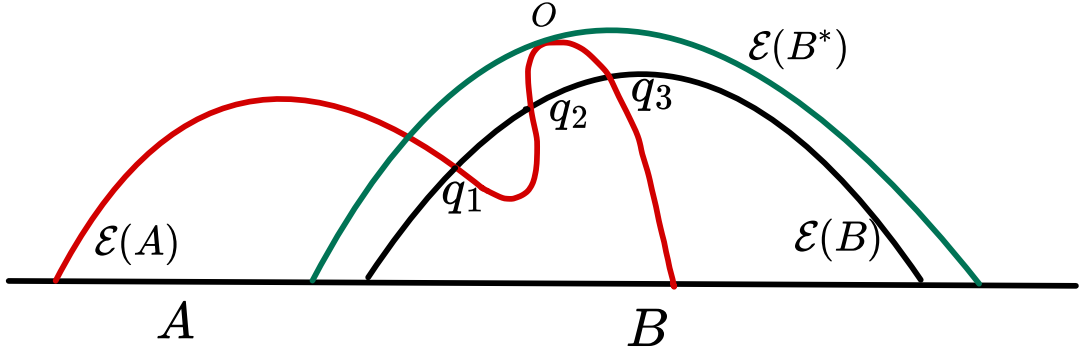


**Figure 1.** Illustration of no multiple entering of HRT surface into another entanglement wedge. The figure shows the Cauchy slice on which the HRT surface of  $A$  (red curve). We also demand  $\Sigma \cap \partial M$  contains the spacelike boundary  $\partial B$  and  $\partial B^*$ . The black and green curves denote  $\partial \mathcal{E}(B) \cap \Sigma$  and  $\partial \mathcal{E}(B^*) \cap \Sigma$ , respectively.

$\partial \mathcal{E}(B)$  must alternate between entering and exiting. Hence the existence of more than one crossing implies the existence of three successive crossing components

$$q_1, q_2, q_3 \subset \gamma_A \cap \partial \mathcal{E}(B),$$

corresponding to an entry into  $\mathcal{E}(B)$ , an exit, and a re-entry. Let  $\mathcal{U}$  denote the open portion of  $\gamma_A$  lying between  $q_2$  and  $q_3$ ; by construction,

$$\mathcal{U} \subset \text{ext } \mathcal{E}(B).$$

*First-contact tangency.* Enlarge  $B$  within the same boundary Cauchy slice to a one-parameter family  $B(\lambda)$  with  $B(0) = B$  and  $B(\lambda_1) \supset B(\lambda_0)$  for  $\lambda_1 > \lambda_0$ . By entanglement wedge nesting,  $\mathcal{E}(B(\lambda_1)) \supset \mathcal{E}(B(\lambda_0))$ . For  $\lambda = 0$  we have  $\mathcal{U} \subset \text{ext } \mathcal{E}(B(0))$ . Increase  $\lambda$  until the first value  $\lambda_* > 0$  for which  $\partial \mathcal{E}(B(\lambda_*))$  meets  $\mathcal{U}$ , and set  $B^* := B(\lambda_*)$ .

By this first-contact construction, there exists a point

$$O \in \mathcal{U} \cap \partial \mathcal{E}(B^*)$$

such that  $\partial \mathcal{E}(B^*)$  is tangent to  $\gamma_A$  at  $O$ , and in a sufficiently small neighborhood of  $O$  the surface  $\gamma_A$  lies entirely on the same side of  $\partial \mathcal{E}(B^*)$ , namely the exterior side of  $\mathcal{E}(B^*)$ . In particular,  $\gamma_A$  intersects  $\partial \mathcal{E}(B^*)$  only at  $O$  in that neighborhood.

*Mean curvature sign on a spatial slice.* The point  $O$  lies on either  $\mathcal{H}^+(B^*)$  or  $\mathcal{H}^-(B^*)$ . Let  $k^\mu$  be the inward-directed null generator of the corresponding horizon component. By the Raychaudhuri equation and the null energy condition, the inward null expansion satisfies  $\theta \leq 0$  along the generators, and by the usual genericity assumption we may take

the first-contact point so that

$$\theta(O) < 0.<sup>1</sup>$$

Choose a bulk Cauchy slice  $\Sigma$  containing  $\gamma_A$ . Since  $\gamma_A$  is extremal, its mean curvature vector in the full spacetime vanishes, and hence  $\gamma_A$  has vanishing mean curvature as a hypersurface in  $\Sigma$ . Deform  $\Sigma$  away from  $O$  so that its second fundamental form is arbitrarily small near  $O$ . Define

$$S_1 := \gamma_A \subset \Sigma, \quad S_2 := \partial\mathcal{E}(B^*) \cap \Sigma.$$

Let  $\nu_{\text{in}}$  denote the unit normal to  $S_2$  in  $\Sigma$  pointing inward into  $\mathcal{E}(B^*)$ . The standard relation between null expansion and spatial mean curvature gives

$$\langle H_{S_2}, \nu_{\text{in}} \rangle = \theta + \mathcal{O}(K^\Sigma),$$

so for  $\Sigma$  chosen as above,

$$\langle H_{S_2}, \nu_{\text{in}} \rangle(O) < 0.$$

*Local strong comparison.* By the first-contact construction,  $S_1$  lies locally on the exterior side of  $S_2$ . Working in local coordinates on  $\Sigma$  near  $O$ , we may represent  $S_1$  and  $S_2$  as graphs over a common domain  $\Omega \subset \mathbb{R}^{d-1}$ ,

$$S_1 = \{(x, u_1(x))\}, \quad S_2 = \{(x, u_2(x))\},$$

with

$$u_1 \leq u_2 \quad \text{in } \Omega, \quad u_1(x_0) = u_2(x_0),$$

where  $x_0$  corresponds to  $O$ .

Let  $\mathcal{M}$  denote the minimal surface operator for graphs with respect to the downward normal, as reviewed in Appendix A. Then  $S_1$  minimal implies  $\mathcal{M}(u_1) = 0$ , while the strict inequality  $\langle H_{S_2}, \nu_{\text{in}} \rangle(O) < 0$  implies  $\mathcal{M}(u_2) < 0$  in a neighborhood of  $x_0$  (after possibly shrinking  $\Omega$ ). Thus locally,

$$\mathcal{M}(u_1) \geq \mathcal{M}(u_2), \quad u_1 \leq u_2, \quad u_1(x_0) = u_2(x_0).$$

By the strong comparison principle for  $\mathcal{M}$  (Proposition A.4), which is a purely local statement, it follows that  $u_1 \equiv u_2$  near  $x_0$ . This would imply that  $\gamma_A$  locally coincides with  $\partial\mathcal{E}(B^*)$ , which contradicts the first-contact set-up.

This contradiction shows that  $\gamma_A$  cannot exit and re-enter  $\mathcal{E}(B)$  along the same connected component. Equivalently,  $\gamma_A$  intersects  $\partial\mathcal{E}(B)$  at most once along each connected component.  $\square$

Below we will repeatedly use the fact that an HRT surface cannot enter and re-enter an entanglement wedge through the same connected component of its horizon (Lemma 2.2).

---

<sup>1</sup> An alternative argument avoids enlarging  $B$  to  $B^*$  and does not require the strict inequality  $\theta(O) < 0$ . One may instead apply a weak maximum principle to the portion of  $\gamma_A$  between  $q_2$  and  $q_3$  and the corresponding portion of  $\partial\mathcal{E}(B)$  on a common Cauchy slice, provided both can be expressed locally as graphs. We do not pursue this variant here.

### 2.3 The “No-Short-Cut” Theorem

For this graph model to capture holographic entropies faithfully, we require  $S^*(I)$  to equal the HRRT entropy  $S(I)$ . A major concern arises because HRRT surfaces for different composite regions do not generally lie on a common Cauchy slice and may even be causally related. This raises the possibility that a graph cut built from an arbitrary collection of partial HRRT surfaces—a “short-cut”—could have a total weight smaller than the area of the actual complete HRRT surface for that region.

For example, with three adjacent regions, could the sum  $|\text{HRT}(A_1A_2) \setminus \mathcal{E}_W(A_2A_3)| + |\text{HRT}(A_2A_3) \setminus \mathcal{E}_W(A_1A_2)|$  be less than  $|\text{HRT}(A_1A_2A_3)|$ ? The following theorem resolves this concern, showing that unions of partial horizons are always suboptimal compared to unions of complete ones.

**Theorem 2.3** (No-Short-Cut). *Let  $W$  be a cut with  $\partial W = I$ , whose corresponding bulk hypersurface  $\gamma$  is a union of segments from various partial entanglement horizons. There exists another cut  $\tilde{W}$  with  $\partial \tilde{W} = I$  whose corresponding hypersurface  $\tilde{\gamma}$  is a union of complete, non-intersecting HRT surfaces. Furthermore,*

$$|C(\tilde{W})| \leq |C(W)|. \quad (2.2)$$

Before presenting the proof of the No-Short-Cut Theorem, we first establish a key lemma that will allow us to project partial HRT surfaces onto a common Cauchy slice with no area increasing.

Given an HRT surface  $\gamma = \text{HRT}(A)$  and a collection of boundary regions  $\{B_i\}$  whose entanglement wedges intersect  $\gamma$ , we define the *outer portion* of  $\gamma$  relative to these wedges by

$$\gamma^\circ := \gamma \setminus \bigcup_i E(B_i).$$

In words,  $\gamma^\circ$  is the part of  $\gamma$  lying outside all entanglement wedges adjacent to  $\gamma$  in the given configuration.

**Lemma 2.4** (Two intersecting entanglement horizons). *Let  $A, B$  be boundary regions with overlapping domains of dependence  $\hat{D}[A] \cap \hat{D}[B] \neq \emptyset$ . Assume the entanglement horizons  $\partial\mathcal{E}(A)$  and  $\partial\mathcal{E}(B)$  intersect. Decompose the corresponding HRT surfaces as*

$$\text{HRT}(A) = \text{HRT}(A)^\circ \cup \text{HRT}(A)^i, \quad \text{HRT}(B) = \text{HRT}(B)^\circ \cup \text{HRT}(B)^i,$$

where the superscripts denote the portions lying outside/inside the other entanglement wedge. Then

$$|\text{HRT}(A)^\circ| + |\text{HRT}(B)^\circ| \geq |\text{HRT}(A \cup B)|. \quad (2.3)$$

*Proof.* Let  $\mathcal{S} = \partial\mathcal{E}(A) \cap \partial\mathcal{E}(B)$  be the intersection seam (see Figure 2 for an illustration). Recall that both  $\partial\mathcal{E}(A)$  and  $\partial\mathcal{E}(B)$  are null hypersurfaces generated by null geodesics with nonpositive expansion toward the interior.

Choose bulk Cauchy slices  $\Sigma_A$  and  $\Sigma_B$  such that  $\text{HRT}(A)$  is minimal on  $\Sigma_A$  and  $\text{HRT}(B)$  and  $\text{HRT}(A \cup B)$  are minimal on  $\Sigma_B$ . By entanglement wedge nesting both slices can be chosen to contain the spacelike boundaries of all relevant boundary regions.,

Consider first the portion  $\text{HRT}(A)^\circ$ . Every point of the seam  $S$  is an endpoint of a null generator emanating from  $\text{HRT}(A)^\circ$ ; otherwise a null generator would enter the interior of  $E(B)$ , contradicting  $\mathcal{H}^-[B] \subset \partial J^-[HRT(B)]$ . Projecting  $\text{HRT}(A)^\circ$  along these generators onto  $\Sigma_B$  therefore does not increase area. An identical argument applies to  $\text{HRT}(B)^\circ$ .

Let  $\tilde{\gamma}$  denote the union of the projected pieces on  $\Sigma_B$ . By construction,  $\tilde{\gamma}$  is homologous to  $A \cup B$ . Since  $\text{HRT}(A \cup B)$  is minimal on  $\Sigma_B$ ,

$$|\text{HRT}(A \cup B)| \leq |\tilde{\gamma}| \leq |\text{HRT}(A)^\circ| + |\text{HRT}(B)^\circ|.$$

This establishes (2.3). □

We now repeatedly use this critical observation of Lemma 2.4 to prove the main Theorem.

*Proof.* We prove the theorem by iteratively simplifying the bulk representative of an arbitrary cut without increasing its area.

Let  $C(W)$  be any cut with boundary  $\partial W = I$ , and let  $\gamma$  denote its bulk representative, assembled from partial pieces of HRT surfaces lying on entanglement horizons  $\partial \mathcal{E}(\cdot)$ . If  $\gamma$  is already a union of complete, non-intersecting HRT surfaces, there is nothing to prove.

Otherwise,  $\gamma$  contains partial pieces lying on at least two intersecting entanglement horizons. By relabeling boundary regions if necessary, we may assume that these include  $\partial \mathcal{E}(A_1 A_2)$  and  $\partial \mathcal{E}(A_2 A_3)$ . Lemma 2.4 shows that in this situation the union of the corresponding outer pieces is dominated by the complete HRT surface  $\text{HRT}(A_1 A_2 A_3)$ . Replacing these pieces therefore weakly decreases the total area and strictly reduces the number of intersecting entanglement horizons involved.

More generally, consider a configuration with several consecutive intersecting entanglement horizons. We repeatedly apply the following local replacement step: select two adjacent intersecting horizons, project the relevant outer pieces onto a common bulk Cauchy slice using null generators, and replace them by the complete HRT surface associated to the union of their boundary regions. This operation is local and depends only on the geometry of the chosen pair of entanglement horizons.

The only subtlety arises from the entanglement wedge nesting structure. When two entanglement horizons, say  $\partial \mathcal{E}(A)$  and  $\partial \mathcal{E}(B)$ , are replaced by the horizon of their union  $\partial \mathcal{E}(A \cup B)$ , entanglement wedge nesting implies that

$$E(A) \cup E(B) \subsetneq E(A \cup B),$$

so the new entanglement wedge generally extends beyond the previous two. As a result, an HRT surface that previously lay outside both  $E(A)$  and  $E(B)$  may partially enter the enlarged wedge  $E(A \cup B)$  and must be modified accordingly.

Concretely, the relevant HRT surface intersects the old entanglement horizon  $\partial \mathcal{E}(A)$  along a codimension-two seam, and after the replacement it must instead intersect the new horizon  $\partial \mathcal{E}(A \cup B)$  along a different seam. The portion of the HRT surface lying on a fixed entanglement horizon that connects two distinct intersection seams with neighboring entanglement horizons is what we call the *bridging piece*. When the union of boundary regions is

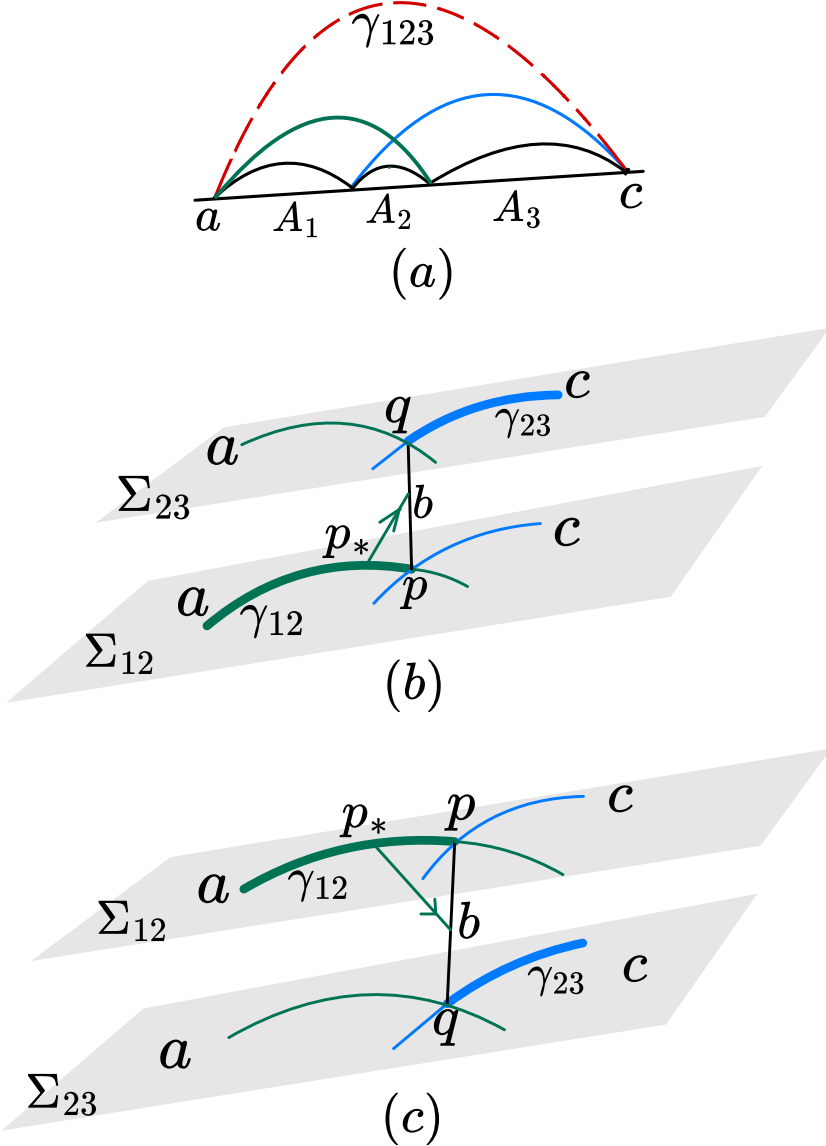


**Figure 2.** Illustration of Lemma 2.4 (two intersecting entanglement horizons) in dimension three. In the notation of the lemma, we identify  $A = A_1 \cup A_2$  and  $B = A_2 \cup A_3$ . Accordingly,  $\partial\mathcal{E}(A)$  and  $\partial\mathcal{E}(B)$  intersect along a seam  $\mathcal{S} = \partial\mathcal{E}(A_1A_2) \cap \partial\mathcal{E}(A_2A_3)$ . Panel (a) shows the configuration projected onto a single time slice. Panel (b) illustrates the projection of the outer portion  $\text{HRT}(A_1A_2) \setminus \mathcal{E}(A_2A_3)$  along null generators onto a common bulk Cauchy slice. Here  $\Sigma_A = \Sigma_{12}$  is a maximin slice on which  $\text{HRT}(A_1A_2)$  is minimal, while  $\Sigma_B = \Sigma_{23}$  is a maximin slice on which both  $\text{HRT}(A_2A_3)$  and  $\text{HRT}(A_1A_2A_3)$  are minimal. The projection replaces two partial HRT surface pieces by a single complete HRT surface  $\text{HRT}(A_1A_2A_3)$  without increasing area. Panel (c) is analogous to Panel (b) and illustrates that the argument does not depend on the relative causal ordering of  $p$  and  $q$ .

enlarged, this same portion of the surface must reconnect to a different intersection seam, changing its boundary attachments while remaining on the same entanglement horizon. A concrete instance of this replacement step is worked out in detail in Section 2.3.1.

To compare the original and modified configurations, one must therefore compare two natural ways of closing this bridge along  $\partial\mathcal{E}(A)$ : one using the old intersection seam and one using the new intersection seam. Applying the same focusing and Stokes-type argument as in the base case to this comparison yields an inequality in which the new seam appears with a negative sign. This negative seam contribution does not reflect an increase of area; rather, it records the fact that the original seam has been traded for the new one when the entanglement wedge is enlarged.

In the subsequent step, the modified HRT surface is projected onto a common bulk Cauchy slice, and this projection produces a positive contribution from precisely the same seam. As shown explicitly in Section 2.3.1, the negative and positive seam terms therefore cancel across successive steps, and the net effect of each local replacement is non-increasing in the total area.

Each replacement strictly reduces the number of intersecting entanglement horizons appearing in  $\gamma$ . Since this number is finite, the procedure terminates after finitely many steps, producing a bulk representative that is a union of complete, non-intersecting HRT surfaces and has area no larger than the original  $\gamma$ .

Finally, if the resulting complete HRT surface is not among those appearing in the graph model, replacing it by the true HRT surface in the same homology class can only further decrease the area. This establishes the theorem.  $\square$

### 2.3.1 A worked example of the induction step

In this subsection we present an explicit example of the local replacement step used in the proof of Theorem 2.3, following the configuration shown in Figure 3. The purpose is to make clear the origin and role of the negative seam contribution that appears at intermediate stages.

Consider three consecutive intersecting entanglement horizons  $\partial\mathcal{E}(A_1A_2A_3)$ ,  $\partial\mathcal{E}(A_2A_3A_4)$ , and  $\partial\mathcal{E}(A_3A_4A_5)$ , with corresponding HRT surfaces

$$\gamma_{123}, \quad \gamma_{234}, \quad \gamma_{345},$$

and let  $\gamma_{2345} = \text{HRT}(A_2A_3A_4A_5)$ . Denote by  $\gamma_{ijk}^o$  the outer portion of  $\gamma_{ijk}$  relative to the neighboring entanglement wedge.

Let  $\Sigma_{345}$  be a bulk Cauchy slice on which  $\gamma_{345}$  is minimal, and let  $\Sigma_{234}$  be a bulk Cauchy slice on which both  $\gamma_{234}$  and  $\gamma_{2345}$  are minimal. Project the outer piece  $\gamma_{345}^o$  from  $\Sigma_{345}$  to  $\Sigma_{234}$  along null generators. As in Lemma 2.4, the focusing theorem and Stokes' theorem imply

$$|\gamma_{345}^o| \geq |\tilde{\gamma}_{345}^o| + |\mathcal{S}_{p_4q_4}|, \quad (2.4)$$

where  $\mathcal{S}_{p_4q_4}$  is the seam segment swept on  $\partial\mathcal{E}(A_2A_3A_4) \cap \partial\mathcal{E}(A_3A_4A_5)$  and  $\tilde{\gamma}_{345}^o = (\partial\mathcal{E}A_3A_4A_5 \cap \Sigma_{234}) \setminus \mathcal{E}(A_2A_3A_4)$  is the projection of  $\gamma_{345}^o$  on  $\Sigma_{234}$ .

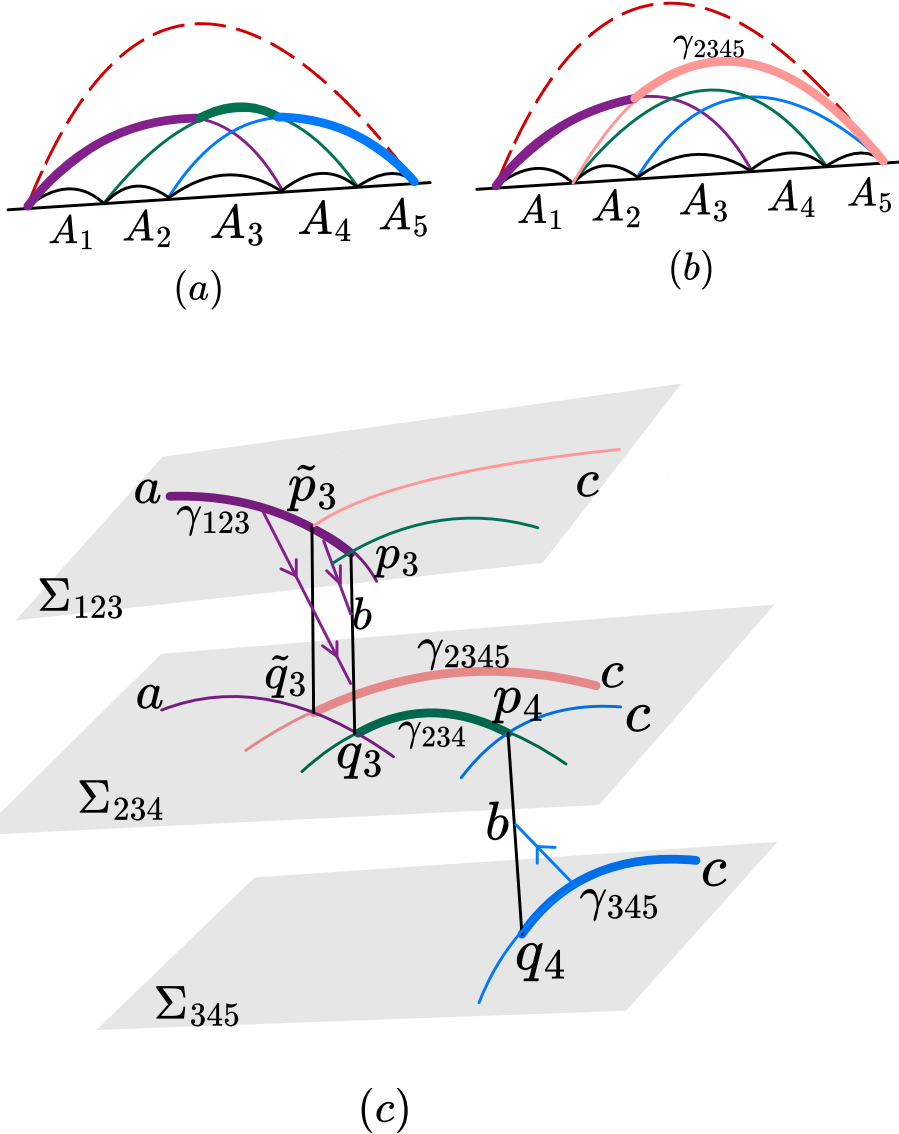


**Figure 3.** Illustration of the induction step in the proof of Theorem 2.3 with three intersecting entanglement horizons in dimension three. Panel (a) illustrates the geometric set-up, suppressing the time direction. Panel (b) highlights the change of partial HRT surfaces before and after the projection step. In particular, the union  $\text{HRT}(A_2A_3A_4) \cup \text{HRT}(A_3A_4A_5)$  (green and blue) is replaced by  $\text{HRT}(A_2A_3A_4A_5)$  (pink). Panel (c) illustrates the projection process along null generators. The thick blue curve  $q_4c$  denotes  $\gamma_{345}^o$ . The thick orange curve  $q_3p_4$  denotes  $\gamma_{234}^o$ . The thick purple curve  $ap_3$  denotes  $\gamma_{123}^o$ . Vertical lines indicate pairwise intersections between entanglement horizons. The bulk Cauchy slice  $\Sigma_{123}$  is a maximin slice for  $\gamma_{123}$ , the bulk Cauchy slice  $\Sigma_{234}$  is a maximin slice for both  $\gamma_{234}$  and  $\gamma_{2345}$ , and the bulk Cauchy slice  $\Sigma_{345}$  is a maximin slice for  $\gamma_{345}$ .

Next we consider the *bridging piece* of  $\gamma_{123}$  on  $\partial\mathcal{E}(A_1A_2A_3)$ , which connects the interface with  $\partial\mathcal{E}(A_2A_3A_4)$  to the interface with  $\partial\mathcal{E}(A_2A_3A_4A_5)$ . There are two natural ways to close this bridge into a closed curve on  $\partial\mathcal{E}(A_1A_2A_3)$ : one uses the old seam on  $\partial\mathcal{E}(A_1A_2A_3) \cap \partial\mathcal{E}(A_2A_3A_4)$ , and the other uses the new seam on  $\partial\mathcal{E}(A_1A_2A_3) \cap \partial\mathcal{E}(A_2A_3A_4A_5)$ . Comparing these two closures via the same focusing/Stokes argument yields

$$|\gamma_{123}^{\text{bridge}}| + |\mathcal{S}_{\text{new}}| \geq |\tilde{\gamma}_{123}^{\text{bridge}}| + |\mathcal{S}_{\text{old}}|. \quad (2.5)$$

Here  $\gamma_{123}^{\text{bridge}}$  and  $\tilde{\gamma}_{123}^{\text{bridge}}$  correspond to the segments  $\tilde{p}_3p_3$  and  $\tilde{p}_3\tilde{q}_3 \cup p_3q_3$  in Figure 3, respectively. The old seam  $\mathcal{S}_{\text{old}}$  and the new seam  $\mathcal{S}_{\text{new}}$  correspond to the segments  $p_3q_3$  and  $\tilde{p}_3\tilde{q}_3$ , respectively.

On the slice  $\Sigma_{234}$ , the surface obtained by joining  $\gamma_{234}^o$ ,  $\tilde{\gamma}_{345}^o$ , and  $\tilde{\gamma}_{123}^{\text{bridge}}$  is homologous to  $A_2A_3A_4A_5$  with the interior inside  $\mathcal{E}(A_1A_2A_3)$  fixed. By minimality of  $\gamma_{2345}$  on  $\Sigma_{234}$ , we have

$$|\gamma_{2345}^o| \leq |\gamma_{234}^o| + |\tilde{\gamma}_{345}^o| + |\tilde{\gamma}_{123}^{\text{bridge}}|. \quad (2.6)$$

Combining (2.4), (2.5), and (2.6), and reattaching the unchanged portion of  $\gamma_{123}$  outside  $\mathcal{E}(A_2A_3A_4A_5)$ , we obtain the explicit inequality

$$|\gamma_{123}^o| + |\gamma_{234}^o| + |\gamma_{345}^o| \geq |\gamma_{123}^{o,\text{new}}| + |\gamma_{2345}^o| - |\mathcal{S}_{\text{new}}|. \quad (2.7)$$

The negative term  $-|\mathcal{S}_{\text{new}}|$  arises precisely because the bridging piece of  $\gamma_{123}$  trades the old seam for the new seam when the union of boundary regions is enlarged. In the next replacement step, this same seam appears with a positive sign when projecting  $\gamma_{123}^{o,\text{new}} := \gamma_{123} \setminus \mathcal{E}(A_2A_3A_4A_5)$  onto a common slice. Thus negative seam contributions are always paired with later positive ones, and the net effect of each local replacement is non-increasing in the total area.

**Remark 2.5.** *Theorem 2.3 guarantees that the minimization defining  $S^*(I)$  reduces to a minimization over cuts corresponding to unions of whole HRT surfaces. This eliminates the short-cut concern and directly ties the graph model entropy to the geometry of entanglement wedge connectivity. A corollary is that the covariant holographic entropy cone, defined via the HRT formula, is isomorphic to the static cone defined via the RT formula. Consequently, all properties derived in [3]—most notably, the polyhedrality of the cone—hold in full generality.*

### 3 Conclusion and Outlook

In this work, we have constructed a graph model for the holographic entropy cone of general time-dependent states. By partitioning the bulk spacetime using entanglement wedges—the fundamental causal constructs of covariant holography—we extended the foundational graph-theoretic framework of Bao et al. beyond time-symmetric slices. The central technical step was proving a general “no-short-cut” theorem (Theorem 1), which leverages entanglement wedge nesting and focusing to show that the discrete entropy minimization reduces to cuts corresponding to unions of complete HRT surfaces.

This result establishes that the holographic entropy cone defined by the covariant HRT formula is identical to the cone derived from the static RT formula. Consequently, all its structural properties—most importantly, its polyhedral nature and the finite basis of linear entropy inequalities—hold universally for holographic states in arbitrary dimensions, irrespective of time dependence.

Our work resolves the obstruction identified in the minimax formulation and provides a concrete geometric interpretation of the abstract complete graph model. It demonstrates that the essential combinatorial structure encoding holographic entanglement is rooted not in a fixed spatial slice, but in the Lorentzian causal architecture of entanglement wedges.

This formulation opens several avenues for future research. One immediate direction is to relax some of the technical assumptions used here, such as the restriction to singularity-free regions and the reliance on maximin existence, and to understand whether the no-short-cut property persists in more general Lorentzian settings. It would also be interesting to explore connections between the present causal graph construction and covariant bit-thread or flow-based formulations of holographic entanglement. Finally, since the holographic entropy cone encodes universal constraints on multipartite entanglement, it is natural to ask whether the covariant perspective developed here can shed light on quantum or semiclassical corrections to these constraints beyond the classical gravity regime.

## Acknowledgments

I thank Edward Witten for introducing this problem to me and for comments on an early draft.

## A A Review of Maximum Principles

### A Maximum Principles and Comparison for the Minimal Surface Operator

In this appendix we collect the versions of the weak and strong maximum principles used in the main text, following the conventions of Leon Simon (see e.g. [11]). We also record the corresponding comparison principles for the minimal surface operator, derived using standard linearization arguments.

#### A.1 Ellipticity and linear operators

Let  $\Omega \subset \mathbb{R}^n$  be a domain and consider a second-order linear operator of the form

$$Lu := \sum_{i,j=1}^n a_{ij}(x) D_i D_j u + \sum_{j=1}^n b_j(x) D_j u + c(x) u. \quad (\text{A.1})$$

We assume:

- $a_{ij}, b_j, c \in L^\infty(\Omega)$ ,
- $a_{ij} = a_{ji}$ ,

- (uniform ellipticity) there exists  $\mu > 0$  such that

$$\sum_{i,j=1}^n a_{ij}(x) \xi_i \xi_j \geq \mu |\xi|^2 \quad \forall x \in \Omega, \xi \in \mathbb{R}^n. \quad (\text{A.2})$$

## A.2 Weak and strong maximum principles

**Theorem A.1** (Weak maximum principle). *Let  $\Omega$  be bounded and let  $u \in C^2(\Omega) \cap C^0(\bar{\Omega})$  satisfy*

$$Lu \geq 0 \quad \text{in } \Omega,$$

where  $L$  is as in (A.1)–(A.2) and

$$c(x) \leq 0 \quad \text{in } \Omega. \quad (\text{A.3})$$

Then

$$\max_{\bar{\Omega}} u \leq \max_{\partial\Omega} u_+, \quad u_+(x) := \max\{u(x), 0\}.$$

If  $c \equiv 0$ , then  $\max_{\bar{\Omega}} u \leq \max_{\partial\Omega} u$ .

**Theorem A.2** (Strong (Hopf) maximum principle). *Let  $\Omega$  be connected and let  $u \in C^2(\Omega)$  satisfy*

$$Lu \geq 0 \quad \text{in } \Omega,$$

with  $L$  as in (A.1)–(A.2) and  $c \leq 0$  in  $\Omega$ . If  $u$  attains a nonnegative maximum at an interior point of  $\Omega$ , then  $u$  is constant in  $\Omega$ . If  $c \equiv 0$ , the qualifier “nonnegative” may be dropped.

## A.3 The minimal surface operator

Let

$$\mathcal{M}(u) := \operatorname{div} \left( \frac{\nabla u}{\sqrt{1 + |\nabla u|^2}} \right) = \sum_{i,j=1}^n \left( \delta_{ij} - \frac{D_i u D_j u}{1 + |Du|^2} \right) \frac{D_{ij} u}{\sqrt{1 + |Du|^2}}.$$

Writing  $\mathcal{M}(u) = \sum_i D_i(A_i(Du))$  with

$$A_i(p) = \frac{p_i}{\sqrt{1 + |p|^2}},$$

we note that

$$\frac{\partial A_i}{\partial p_j}(p) = \frac{\delta_{ij}}{\sqrt{1 + |p|^2}} - \frac{p_i p_j}{(1 + |p|^2)^{3/2}}$$

is positive definite. Thus  $\mathcal{M}$  is quasilinear elliptic and corresponds, upon linearization, to an operator  $L$  of the form (A.1) with  $c \equiv 0$ .

Geometrically, if  $u$  is a graph over  $\Omega \subset \mathbb{R}^n$  and

$$\nu := \frac{(\nabla u, -1)}{\sqrt{1 + |\nabla u|^2}}$$

denotes the *downward-pointing* unit normal to the graph, then

$$\mathcal{M}(u) = \operatorname{div}(\nu).$$

With this convention,  $\mathcal{M}(u) = 0$  is equivalent to vanishing mean curvature. Moreover, if a smooth hypersurface is strictly mean-convex with respect to the *upward* normal, then when written locally as a graph with downward normal it satisfies  $\mathcal{M}(u) < 0$ . In particular, an upper hemisphere written as a graph over its tangent plane at the north pole satisfies  $\mathcal{M}(u) < 0$ , while the tangent plane itself satisfies  $\mathcal{M}(u) = 0$ .

#### A.4 Weak comparison principle for $\mathcal{M}$

**Proposition A.3** (Weak comparison). *Let  $\Omega$  be bounded and suppose*

$$\mathcal{M}(u_1) \leq \mathcal{M}(u_2) \quad \text{in } \Omega,$$

*with  $\mathcal{M}(u_i) \in C^0(\bar{\Omega})$ . Assume*

$$u_1 = u_2 \quad \text{on } \partial\Omega.$$

*Then*

$$u_2 \leq u_1 \quad \text{in } \Omega.$$

*Proof.* Set  $w := u_2 - u_1$ . Writing  $\mathcal{M}(u) = \sum_i D_i(A_i(Du))$ ,

$$\mathcal{M}(u_2) - \mathcal{M}(u_1) = \sum_{i,j} D_i(a_{ij}(x)D_j w),$$

where

$$a_{ij}(x) = \int_0^1 \frac{\partial A_i}{\partial p_j}(Du_1 + tD(u_2 - u_1)) dt.$$

The matrix  $(a_{ij})$  is uniformly elliptic. Since  $\mathcal{M}(u_2) - \mathcal{M}(u_1) \geq 0$ , we obtain

$$\sum_{i,j} a_{ij} D_i D_j w + \sum_i D_i(a_{ij}) D_j w \geq 0.$$

Thus  $w$  satisfies  $Lw \geq 0$  with  $c \equiv 0$  and  $w = 0$  on  $\partial\Omega$ . The weak maximum principle yields  $w \leq 0$  in  $\Omega$ .  $\square$

#### A.5 Strong comparison principle for $\mathcal{M}$

**Proposition A.4** (Strong comparison). *Let  $\Omega$  be connected and suppose*

$$\mathcal{M}(u_1) \leq \mathcal{M}(u_2) \quad \text{in } \Omega, \quad u_1 \geq u_2 \quad \text{in } \Omega.$$

*If there exists  $x_0 \in \Omega$  such that  $u_1(x_0) = u_2(x_0)$ , then*

$$u_1 \equiv u_2 \quad \text{in } \Omega.$$

*Proof.* With  $w := u_2 - u_1$  as above, we obtain  $Lw \geq 0$  with  $c \equiv 0$ . The hypotheses give  $w \leq 0$  in  $\Omega$  and  $w(x_0) = 0$ . By the strong maximum principle (Theorem A.2),  $w$  is constant, hence  $w \equiv 0$ .  $\square$

## A.6 Geometric interpretation

Proposition A.4 is equivalent to the geometric statement that a minimal graph cannot touch, from the side on which it lies, another graph whose mean curvature vector (computed with respect to the same choice of normal) points strictly away from it, unless the two coincide locally. In particular, the tangent plane at a point of a strictly mean-convex surface does not violate the principle, since the required inequality on mean curvatures fails in that case.

## B Geometric Interpretation of the Complete Graph

We provide a geometric interpretation of the complete graph with vertex set  $\mathcal{V} = \{0, 1\}^{\mathcal{P}(\{1, \dots, n\}) \setminus \emptyset}$ , which was introduced algebraically in [3] to represent the entropy cone. Each entanglement horizon  $\text{HRT}(A_I)$  divides the bulk into two parts. A bitstring  $x \in \mathcal{V}$  can be interpreted as indicating, for each composite region  $I$ , whether a given spacetime point is "inside" ( $x_I = 1$ ) or "outside" ( $x_I = 0$ ) the corresponding entanglement wedge. The vertex  $x_i$  defined by  $(x_i)_I = 1 \iff i \in I$  corresponds precisely to the bulk region causally connected to boundary  $A_i$ —that is, its entanglement wedge. Considering all  $2^n - 1$  possible composite regions and their associated (fully connected) extremal surfaces yields the finest possible partition of the bulk spacetime, naturally recovered by this complete set of bitstrings. This perspective elucidates the constructions in Lemma 6 and Proposition 7 of [3], framing them not as abstract combinatorial choices but as consequences of spacetime causality and wedge structure.

## References

- [1] S. Ryu and T. Takayanagi, *Holographic derivation of entanglement entropy from the anti-de sitter space/conformal field theory correspondence*, *Physical review letters* **96** (2006) 181602.
- [2] V.E. Hubeny, M. Rangamani and T. Takayanagi, *A covariant holographic entanglement entropy proposal*, *Journal of High Energy Physics* **2007** (2007) 062.
- [3] N. Bao, S. Nezami, H. Ooguri, B. Stoica, J. Sully and M. Walter, *The holographic entropy cone*, *Journal of High Energy Physics* **2015** (2015) 1.
- [4] B. Grado-White, G. Grimaldi, M. Headrick and V.E. Hubeny, *Minimax surfaces and the holographic entropy cone*, *Journal of High Energy Physics* **2025** (2025) 1.
- [5] A.C. Wall, *Maximin surfaces, and the strong subadditivity of the covariant holographic entanglement entropy*, *Classical and Quantum Gravity* **31** (2014) 225007.
- [6] A. May, G. Penington and J. Sorce, *Holographic scattering requires a connected entanglement wedge*, *Journal of High Energy Physics* **2020** (2020) 1.
- [7] C. Lima, S. Pasterski and C. Waddell, *On sufficient conditions for holographic scattering*, *arXiv preprint arXiv:2509.26264* (2025) .
- [8] B. Zhao, *A proof of the generalized connected wedge theorem*, *Journal of High Energy Physics* **2026** (2026) 29.
- [9] B. Zhao, *Beyond 2-to-2: Geometrization of entanglement wedge connectivity in holographic scattering*, *arXiv preprint arXiv:2512.06815* (2025) .

- [10] R.M. Wald, *General relativity*, University of Chicago press (2024).
- [11] L. Simon, “Lectures on PDE.” 2022.